JOURNAL OF AIRCRAFT
Vol. 29, No. 5, Sept.–Oct. 1992

Model Flight Tests of a Spin-Resistant Trainer Configuration

Long P. Yip,* Holly M. Ross,† and David B. Robelen‡
NASA Langley Research Center, Hampton, Virginia 23665

Powered, radio-controlled flight tests were conducted on a ¼-scale model of a spin-resistant trainer configuration to determine the stall departure and spin resistance characteristics provided by an outboard wing leading-edge droop modification. The model was instrumented to provide quantitative as well as qualitative information on flight characteristics. Flight test results indicated that the unmodified configuration (wing leading-edge droop off) exhibited an abrupt, uncontrollable roll departure at the stall. With the outboard wing leading-edge droop installed, the modified configuration exhibited flight characteristics that were resistant to stall departure and spin entry. The stall departure and spin resistance characteristics of the modified configuration were demonstrated in flight maneuvers that included idle-power stalls, full-power stalls, sideslip stalls, and accelerated stalls. In addition, limited quantitative flight data were obtained at various center-of-gravity locations and power settings with the model trimmed for level flight conditions in order to assess some basic aerodynamic and stability and control characteristics. The model flight results were generally in good agreement with previously obtained wind-tunnel data.

Nomenclature

b = wing span, ft
C_L = lift coefficient, lift/qS
c = local chord, ft
$\bar{c}$ = wing mean aerodynamic chord, ft
q = freestream dynamic pressure, lb/ft
S = wing reference area, ft²
α = angle of attack, deg
β = angle of sideslip, deg
δ_a = aileron deflection, (left–right)/2, positive for left roll, deg
δ_e = elevator deflection, positive trailing-edge down, deg
δ_r = rudder deflection, positive trailing-edge left, deg

Introduction

DURING the late 1970s and into the 1980s, the stall/spin research program at the NASA Langley Research Center had produced new techniques for improving the stall departure and spin resistance characteristics of general aviation aircraft. Much of this effort has been focused on the influence of wing aerodynamics on the stall and departure characteristics of these airplanes. Results from wind tunnel and flight tests have shown that a wing leading-edge droop modification can provide attached flow on the outer wing panel to angles of attack well beyond the normal wing stall angle of attack, and thus improve the configuration's stall departure characteristics.[1–4] This modification generally consisted of a drooped leading edge on the outboard wing panel with a sharp discontinuity at the inboard edge of the droop.

A cooperative research program was undertaken with the DeVore Aviation Corporation to study the outboard wing leading-edge droop concept on a spin-resistant trainer configuration. As part of the cooperative effort, a wind-tunnel investigation had been conducted on a ⅙-scale model of this configuration to determine the effects of wing leading-edge modifications on the high-angle-of-attack characteristics, and the results were reported in Ref. 5. From the wind-tunnel investigation, an outboard wing leading-edge droop modification was found to significantly increase stall protection on the outer wing panel and to improve roll damping and lateral control authority at high angles of attack.

Following the wind tunnel investigation, powered radio-controlled flight tests were conducted on a ¼-scale model (Fig. 1) of the trainer configuration in order to obtain flight characteristics which would augment the aerodynamic data obtained from the wind-tunnel investigation. The model was tested with and without the outboard wing leading-edge droop modification installed. The objectives of this investigation were to determine the effectiveness of the wing leading-edge modification in flight at high angles of attack and to correlate flight results with wind-tunnel data. The purpose of this article is to report the results of the model flight test investigation.

Model Description

The ¼-scale, powered, radio-controlled model, shown in Fig. 1, was geometrically similar to the ⅙-scale wind tunnel model reported in Ref. 5. However, some modifications were made to the radio-controlled model based on results of the wind-tunnel investigation. These configuration changes included increasing the horizontal tail area, adding dorsal and ventral fin areas on the tail boom, and adding vortex generators on the sides of the aft-fuselage areas. A three-view

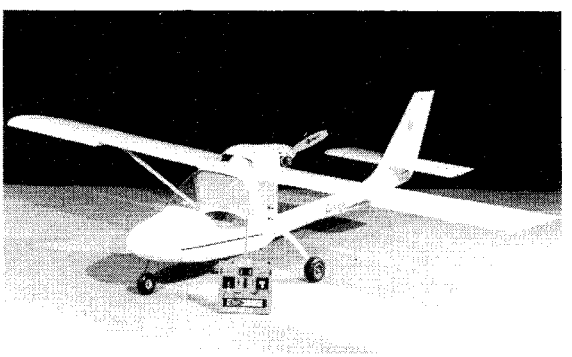

Fig. 1 Three-quarter front view of one-fourth-scale powered, radio-controlled model.

Presented as Paper 88-2146 at the AIAA 4th Flight Test Conference, San Diego, CA, May 18–20, 1988; received July 13, 1990; revision received Sept. 1, 1991; accepted for publication Sept. 26, 1991.

*Research Engineer, Flight Research Branch, Flight Applications Division, Mail Stop 247. Senior Member AIAA.
†Research Engineer, Flight Dynamics Branch, Flight Applications Division, Mail Stop 355. Member AIAA.
‡Engineering Technician, Operations Support Division, Mail Stop 355.

sketch of the configuration is shown in Fig. 2. The configuration is defined by its two-placed side-by-side seating, pusher propeller location, tail-boom stabilizer section, tricycle landing-gear arrangement, and its outboard wing leading-edge droop modification for stall departure and spin resistance. The model has an aspect ratio 7.8 wing with an untwisted, constant chord wing planform and a NACA 64(1)-212 MOD B wing section.[6] A comparison of the drooped airfoil section and the basic airfoil section is shown in Fig. 3.

The model was dynamically scaled for flight tests in accordance with the methods of Ref. 7. A scale factor of $\frac{1}{4}$ was chosen so that the model would be large enough to make flying qualities acceptable for research, yet small enough to allow for the use of existing hobby-type equipment such as transmitters, receivers, servos, and engines. The model was ballasted with lead weight in the nose in order to balance the model for more forward center-of-gravity locations. The center-of-gravity locations tested and the corresponding model weights are listed in Table 1. Moments-of-inertia characteristics are listed in Table 2. The model was constructed so that the leading-edge section of the basic airfoil could be replaced with the leading-edge droop modification on the outboard panel of the wing. The model had a simple-hinged, trailing-edge flap which could be deflected to 40 deg. Maximum control deflections were 15 deg trailing-edge down and 30 deg trailing-edge up for elevators, 15 deg trailing-edge down and 25 deg trailing-edge up for ailerons, and 25 deg trailing-edge left and right for the rudder. The model was powered by a hobby-type aircraft engine that developed approximately 3.0 horsepower.

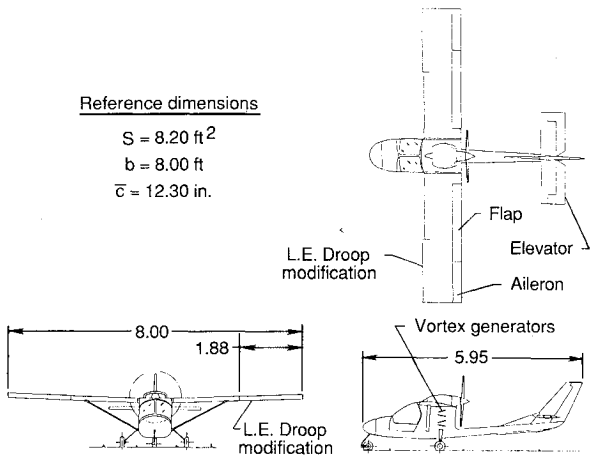

Fig. 2 Three-view sketch of model. Dimensions in feet.

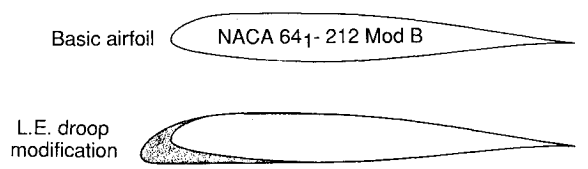

Fig. 3 Comparison of basic airfoil with leading-edge droop modification.

Table 1 Model weight and c.g. characteristics

Center-of-gravity, percent $\bar{c}$	Take-off gross weight, lbs
25.00	22.80
30.00	22.05
35.00	21.38
40.00	20.73

Table 2 Model inertia characteristics: c.g. at 25% c

Axis	Moments of inertia, slug-ft²
Pitch	1.96
Roll	0.81
Yaw	2.13

Test Facility

Powered, radio-controlled model tests were conducted at the NASA Plum Tree Test Site located near Poquoson, Virginia. The Plum Tree Test Site consists of two runways of approximately 50 ft in width and 275 ft in length for takeoff and landing of the model. A manually operating tracking unit, shown in Fig. 4, was used in the process of video recording each flight. Mounted on the tracking unit is a broadcast-grade video camera with a variable zoom lens capable of a 22× magnification factor. A separate area was used to house the video recording equipment and to conduct the video recording operations. A more detailed description of the test facility can be found in Ref. 8.

Instrumentation and Data Reduction

The overall test setup for radio-controlled model tests is illustrated in Fig. 5. A telemetry transmitter with up to seven channels of onboard instrumentation data is transmitted to a receiving unit on the ground. In addition, the seven channels of pilot input data that is transmitted to control the model is also received on the ground as well. Both the on-board telemetry transmitter signals and the pilot's control command transmitter signals are received on the ground control unit,

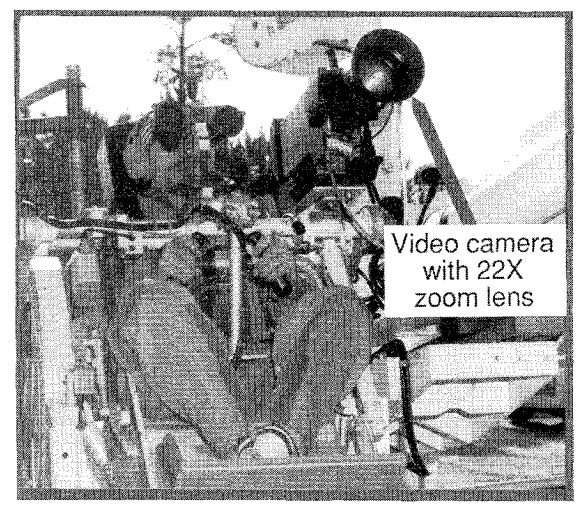

Fig. 4 Camera tracking unit.

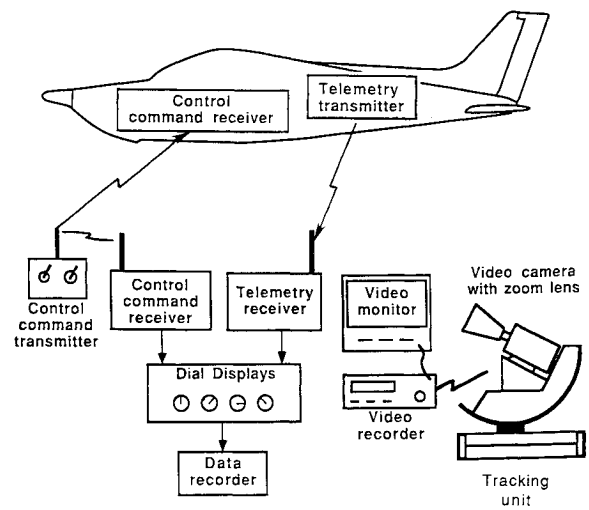

Fig. 5 Test setup for radio-controlled model tests.

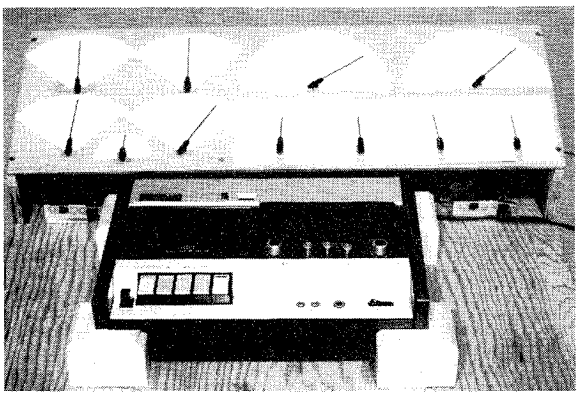

Fig. 6 Ground control unit for data acquisition.

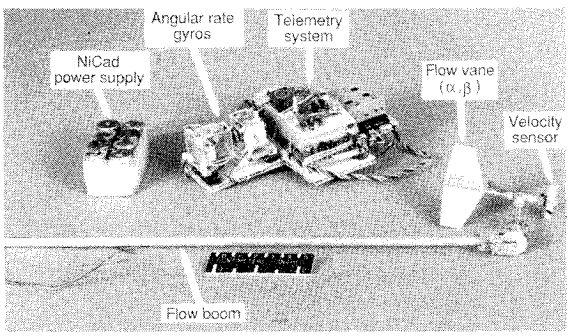

Fig. 7 Instrumentation for radio-controlled model tests.

shown in Fig. 6. The data were sampled at a rate of 60 data frames per second. The transmitted signals activate hobby-type servos which were used as simple dial gauges to monitor key parameters in engineering units in real time. The signals were also recorded on a modified audio cassette tape recorder for data playback and later processed through an analog-to-digital conversion for data analysis.

Typically, key parameters measured include the angles of attack and sideslip; airspeed; angular rates in roll, pitch, or yaw; engine rpm; and control positions from the onboard instrumentation. From the control transmitter, key parameters recorded include pilot control positions of the elevator, ailerons, and rudder; power setting; flap position; and event marks which define test segments on the data recording tape. Because of the restrictions in model weight and the limited number of data recording channels, key parameters were selectively reduced to conserve time and space in the data reduction process. For this investigation, the $\frac{1}{4}$-scale radio-controlled model was instrumented for angle of attack, angle of sideslip, velocity, roll rate, and engine rpm.

Figure 7 shows the instrumentation used on this flight test. Much of the instrumentation was developed by utilizing and modifying low-cost, hobby-type equipment. A miniature velocity sensor, consisting of a multibladed turbine, was built, and the calibration was done in a small calibration wind tunnel to determine true airspeed. The velocity sensor was incorporated into the flow vane which measures angles of attack and sideslip. The flow direction/velocity sensor was mounted on a flow boom and was installed in front of the model's nose in order to minimize the influence of the body on the free-stream flowfield.

Lift coefficients were computed from flight data at trimmed level flight conditions knowing the test conditions of model airspeed, atmospheric conditions, and model weight. Atmospheric conditions of barometric pressure and temperature were recorded prior to each flight in order to compute the density of the air for use in the reduction of flight data into coefficient form. The model gross takeoff weight was recorded prior to each flight, and the model weight during flight was computed based on the approximate fuel used at a given flight time.

Flight data were telemetered to a ground station, and audio-ovisual recordings were documented each flight. Control position data were obtained by calibrating and recording stick movement on the command transmitter. Strip chart readings of the various data channels provided flight data for each of the flight maneuvers. In addition to quantitatively recorded data from the test flights, audio-video recordings are made using a broadcast quality video cassette recorder along with the precision tracking equipment located at the Plum Tree Test Site. The qualitative data recorded on video tape provided valuable test information in terms of pilot comments and visual aircraft motions for each of the flight maneuvers performed. These audio-video recordings were essential in correlating and interpreting the quantitative data recorded.

Test Procedures

Flight test emphasis was placed on the assessment of stall departure resistance on the unmodified and the modified wing configurations. The radio-controlled model was flown at various center-of-gravity locations from 25 to 40% of the mean aerodynamic chord.

Model flight tests consisted of a ground takeoff, a climb to test altitudes, and flight in an oval pattern so that the model was always in front of the pilot and ground tracking unit for each of the flight test segments. Using the spin resistance criteria developed in Refs. 9 and 10, the following flight maneuvers were performed to assess stall departure resistance of the configuration:

1) *Idle power stall*—The model was flown with the wings level and power reduced to idle. The stick was gradually pulled back and was held full back with minimal aileron and rudder inputs to maintain heading.

2) *Uncoordinated sideslip stalls*—The model was flown with power reduced to idle. The stick was gradually pulled back and was held, and the rudder was deflected full left or right to generate sideslip. Opposite aileron inputs were applied to maintain heading.

3) *Lateral response*—At idle power, the stick was gradually pulled to full back and was held. From a wings level flight condition, ailerons were applied to roll the model from a left bank to a right bank of approximately 30 deg and then back to wings level.

4) *Full-power stall*—This maneuver was similar to the idle power maneuver, except that full power was gradually applied and maintained throughout the stall.

5) *Accelerated stall with full power*—The model was banked to 45 deg with full power, and the stick was gradually pulled back. The flight maneuver was repeated for the opposite (left or right) turn direction.

In addition to the stall maneuvers, the following flight maneuvers were performed to obtain some basic aerodynamic and stability and control characteristics of the configuration:

1) *Trimmed level flight*—Starting with full power, the model was trimmed for several low, level passes along the runway. Each pass was made with a reduced power setting to acquire trimmed flight data at various velocity conditions.

2) *Trimmed level flight at sideslip*—For trimmed level flight, the rudder was deflected to generate a sideslip condition, and aileron inputs were applied to maintain heading.

3) *Elevator doublet*—With the model in trimmed level flight, the model was oscillated in pitch with quick elevator inputs and released to the trimmed setting to determine the longitudinal damping of the configuration.

4) *Rudder doublet*—This maneuver was similar to the elevator doublet except that rudder inputs were applied to determine the lateral-directional damping characteristics.

Results and Discussion

Stall Departure and Spin Resistance Characteristics

A series of flight maneuvers, described earlier, were performed to assess the configuration's stall departure and spin

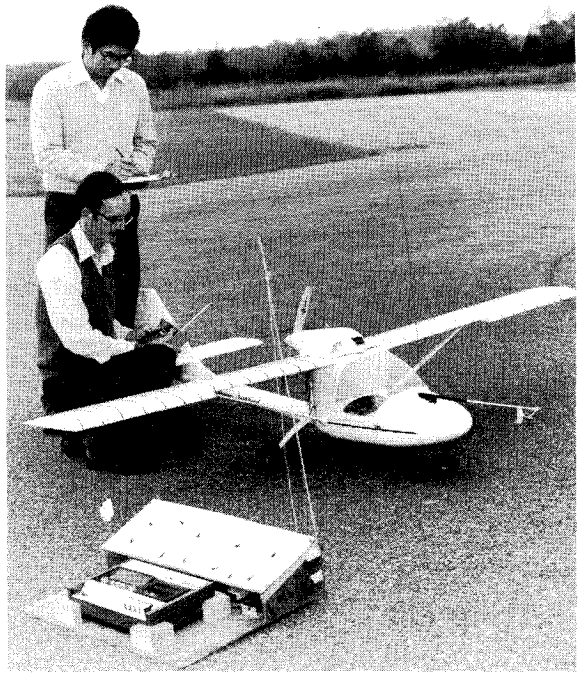

Fig. 8 Instrumented model at test site.

resistance characteristics. The instrumented model, shown in Fig. 8, was flown with and without the wing leading-edge droop modification. The roll rate data are presented without scales due to calibration uncertainties. However, the data are presented because the data trends were useful in the analysis of the model's flight characteristics.

Test results of the idle power stall maneuver for the basic wing configuration are presented in Fig. 9 in the form of time history traces for angle of attack, angle of sideslip, velocity, elevator position, and roll rate. The flight maneuver was conducted at a center of gravity location of 25% of the mean aerodynamic chord. The time history traces of Fig. 9 indicate that when the stick was pulled back, as indicated by the elevator deflection, the angle of attack increased, and the velocity decreased during the initial part of this maneuver. With increasing aft-stick movement, the basic unmodified model exhibited an abrupt, uncontrollable roll departure at full aft-stick elevator control. The roll departure is indicated by the large change in roll rate at about the 13-s time mark. The angle of attack at the onset of departure was about 16 deg. This departure angle of 16 deg measured from model flight is in agreement with the wing-stall angle measured from the wind tunnel.

Figure 10 shows model flight data for the idle power stall maneuver on the modified configuration with the outboard wing leading-edge droop installed. The model flight data are presented with the model center of gravity (c.g.) at an aft location of 35% mean aerodynamic chord. Even though flight characteristics were more sensitive with aft c.g. movement, visual observations of the flight indicated that the modified model did not exhibit any abrupt departure even with the control stick held full aft for about 12 s. The data did show, however, that the model was unsteady in roll about a wings level attitude in this post-stall condition. Angle of attack reached about 25 deg, which is significantly higher than that attained for the unmodified configuration. Roll oscillations of the model are shown in the sideslip and roll rate data traces while the model was flying in this post-stall condition. These oscillations were probably caused by reduced roll damping and the wake shedding from the aft-body/wing combination onto the vertical tail area of these post-stall, high angles of attack conditions.

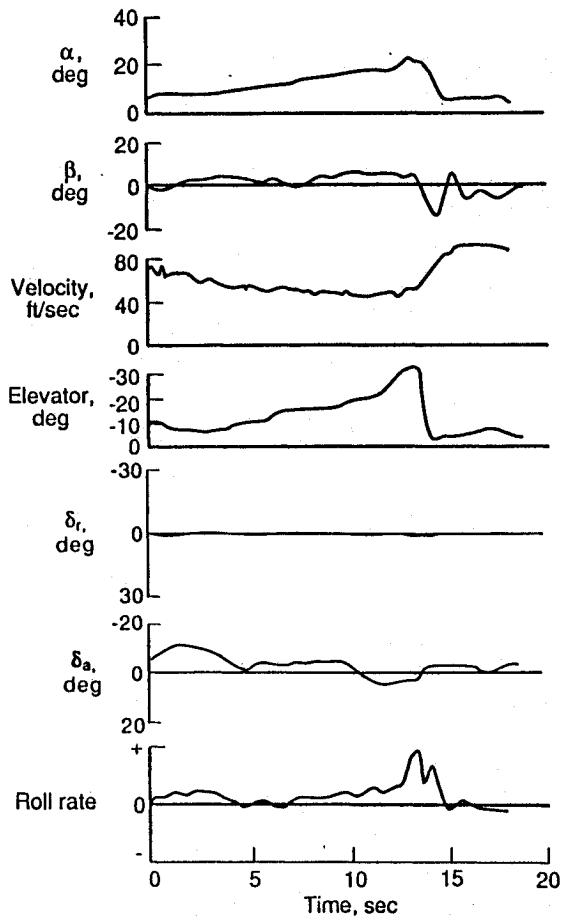

Fig. 9 Model flight data. Idle power stall, leading edge (L.E.) droop off, c.g. at 25% $\bar{c}$.

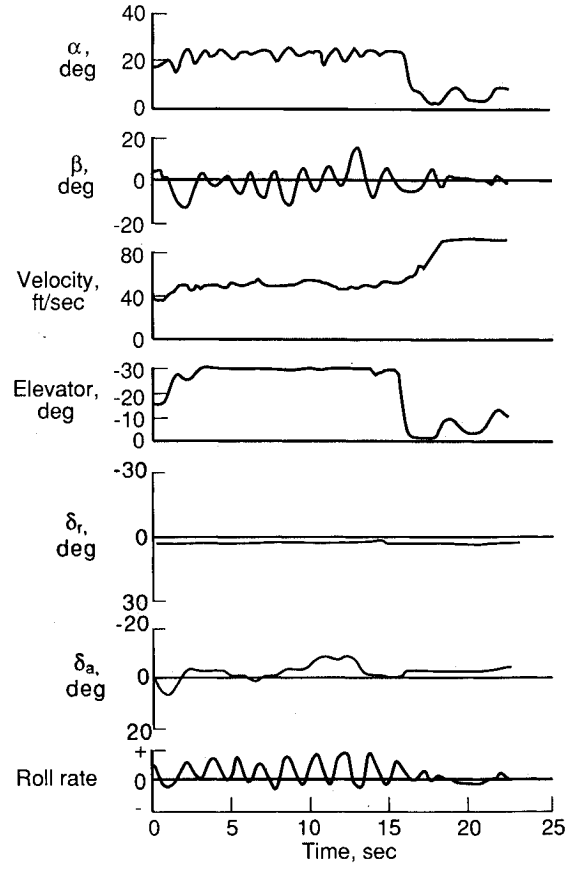

Fig. 10 Model flight data. Idle power stall, L.E. droop on, c.g. at 35% $\bar{c}$.

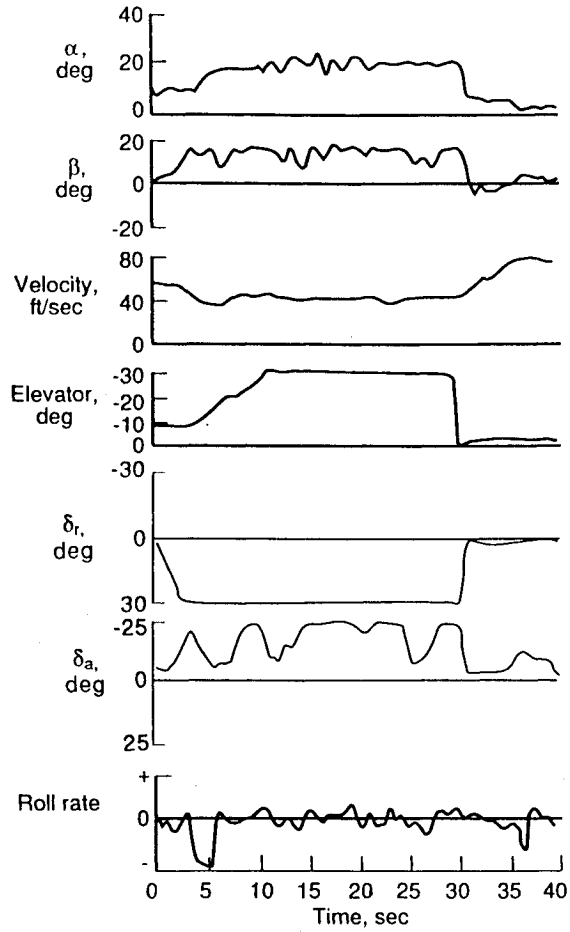

Fig. 11 Model flight data. Idle power stall, full left rudder, L.E. droop on, c.g. at 25% $\bar{c}$.

Figure 11 shows model flight data for the uncoordinated stall maneuver on the modified leading-edge droop configuration. The flight was conducted at a center of gravity of 25% mean aerodynamic chord, and full left rudder was applied at the stall using opposite aileron input to maintain heading. As indicated by the data of Fig. 11, the angle of attack increased with increasing elevator deflection. An angle of attack of 23 deg and an angle of sideslip of 15 deg were attained during this flight maneuver. No departures were observed for the modified leading-edge droop configuration in this uncoordinated stall maneuver. However, near the beginning of the flight, the data indicated a change in roll rate at about the 3-s mark. Based on flow visualization studies from the wind tunnel investigation of Ref. 5, the inboard wing panel exhibited an abrupt stall while the outboard wing panel flow remained attached. This abrupt change in roll rate could be explained by an initial asymmetric stall of the inboard wing panel due to sideslip while the model increased in angle of attack. Since the flow on the modified outer wing panel was attached, aileron control power was maintained, and therefore, the roll-off was controlled with corrective aileron inputs.

Aileron control power at stall and post-stall conditions was further investigated by observing the model response in the lateral response flight maneuver described previously. Flight test results indicated that the ailerons had sufficient control power to bank the model from left to right and back to wings level at full aft stick post-stall conditions.

Model flight data for the full-power stall condition are shown in Fig. 12 for the modified droop configuration at an aft center of gravity location of 35% mean aerodynamic chord. Visual observations of the test flight indicated that the modified leading-edge droop configuration did not exhibit stall departure with full aft stick and full power settings. The data indicated that the maximum angle of attack attained was about 22 deg, which is less than the maximum angle of attack achieved by the idle power maneuver. The lower angle of attack at full power is probably caused by the high thrust line which produces an offset in nose-down pitching moment.

Figure 13 shows model flight data fron an accelerated stall maneuver with full power for the modified droop configuration. The center of gravity for this flight was located at 25% mean aerodynamic chord. Visual observations indicated that the modified configuration did not exhibit a stall departure for this accelerated stall flight maneuver with full aft stick and full power setting.

Additional flights to assess stall departure resistance characteristics at center of gravity locations of 30 and 40% mean aerodynamic chord were also performed on the modified droop configuration. From flight observations, the modified leading-edge droop configuration did not exhibit stall departure in any of the stall flight maneuvers performed.

Flight Characteristics at Low Angles of Attack

Trimmed level flights for a range of velocity and power settings were conducted at various c.g. locations to obtain basic stability and control data. The model was also perturbed from trimmed flight in either the longitudinal or lateral-directional axes to assess the damping motions of the model.

The elevator deflection required for trimmed level flight on the modified configuration is shown in Fig. 14 for various

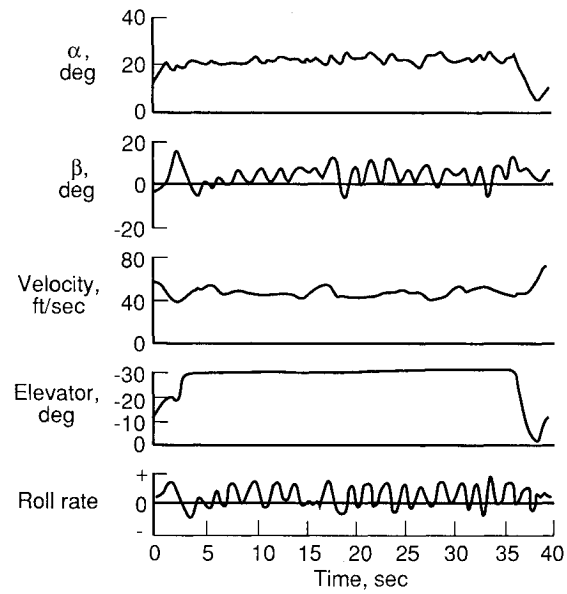

Fig. 12 Model flight data. Full power stall, L.E. droop on, c.g. at 35% $\bar{c}$.

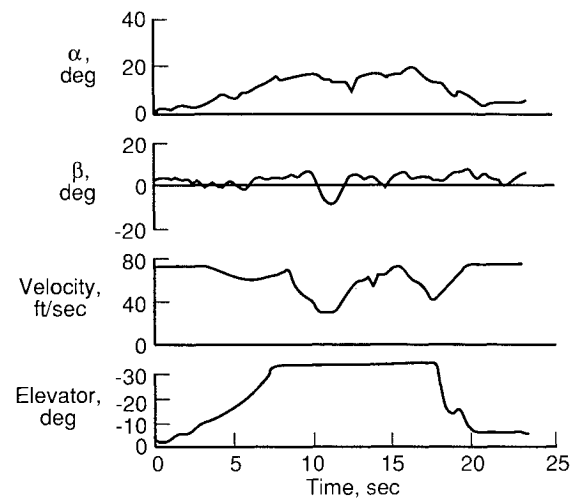

Fig. 13 Model flight data. Accelerated left turn stall, L.E. droop on, c.g. at 25% $\bar{c}$.

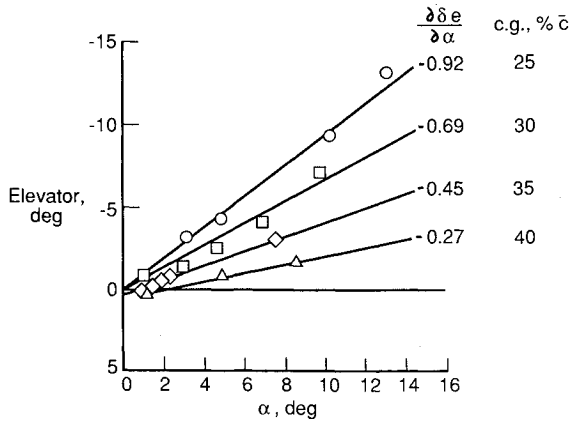

Fig. 14 Elevator deflection required for trimmed level flight. L.E. droop on.

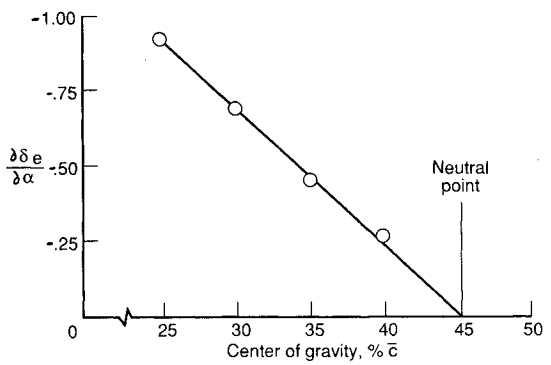

Fig. 15 Stability and control characteristics from model flight data. L.E. droop on.

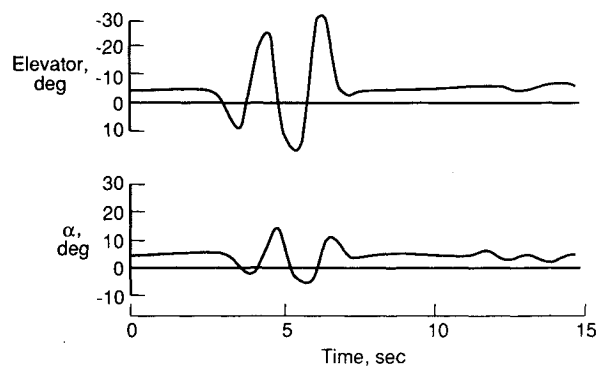

Fig. 16 Model flight data. Pitch oscillation maneuver, L.E. droop on, c.g. at 25% $\bar{c}$.

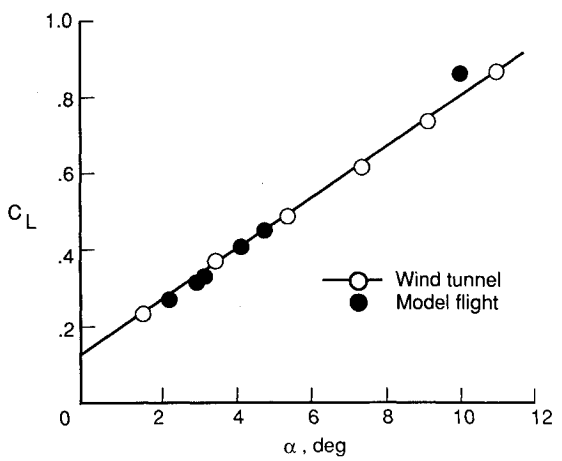

Fig. 17 Comparison of model flight data with wind-tunnel data. L.E. droop on.

center-of-gravity locations. As expected, the data indicate that the elevator is more sensitive in trim as the center of gravity is moved aft. Linearized values of $\partial\delta_e/\partial\alpha$ are plotted against center of gravity location in Fig. 15. By extrapolating the data of Fig. 15, an estimate of the neutral point can be made. The neutral point estimate based on the intercept value where $\partial\delta_e/\partial\alpha = 0$ is shown to be located at the 45% mean aerodynamic chord of the modified droop configuration. The neutral point estimate extracted from model flight data compares well with the neutral point estimate of 44% mean aerodynamic chord from wind-tunnel data.

Figure 16 shows time history traces of the elevator doublet maneuver performed on the modified droop configuration with a center-of-gravity location of 25% mean aerodynamic chord. As shown by the data, model aircraft motions were excited by rapid elevator oscillations. Changes in angle of attack closely followed the movement at elevator deflection. As the elevator motion was stopped, aircraft motions in pitch were quickly damped. Observed aircraft motions using rudder inputs also indicated that the configuration was highly damped in the lateral-directional axes.

Comparison of Flight with Wind-Tunnel Data

Trimmed flight data are shown in Fig. 17 in the form of lift coefficient against angle of attack. The wind tunnel lift data of Ref. 5 are also plotted for comparison. Although separate models having similar geometry were used for each investigation, good agreement was obtained between wind-tunnel and model-flight data at the low to moderate angles of attack. The agreement between flight and wind-tunnel data was good in terms of the lift curve slope and in terms of the magnitude of the lift values.

Summary of Results

A flight investigation was conducted on an instrumented, ¼-scale powered, radio-controlled model of an advanced trainer configuration to determine the stall departure and spin-resistance characteristics of the configuraton. From a previous wind-tunnel investigation, a wing leading-edge droop modification was developed for the model to provide improved stall departure resistance. The major results of the model flight test investigation are summarized as follows:

1) The configuration with the unmodified wing exhibited an abrupt, uncontrollable departure in flight with full aft-stick control input.

2) With the outboard wing leading-edge droop modification, the configuration exhibited departure resistance at angles of attack significantly beyond the normal stall angle. Departure resistance was demonstrated on the modified configuration for flight maneuvers including stalls with aft center of gravity location uncoordinated stalls at sideslip conditions, stalls with full-power setting, and accelerated stalls in turning flight.

3) Lateral control of the modified configuration at the stall was maintained in left-to-right banking maneuvers with full aft stick input.

4) From analysis of flight data, the neutral point was determined to be located at 45% of the mean aerodynamic chord. The flight-determined neutral point was in good agreement with previously reported wind-tunnel data.

5) Lift coefficients reduced from model flight data were in good agreement with wind-tunnel lift data in the low to moderate angle-of-attack range.

References

[1]Anon., "Exploratory Study of the Effects of Wing Leading-Edge Modifications on the Stall/Spin Behavior of a Light General Aviation Airplane," NASA TP 1589, 1979.

[2]Newsom, W. A., Satran, D. R., and Johnson, J. L., Jr., "Effects of Wing Leading-Edge Modifications of a Full-Scale Low-Wing General Aviation Airplane," NASA TP 2011, June 1982.

[3]Stough, H. P., III, DiCarlo, D. J., and Stewart, E. C., Wing

Modification for Increased Spin Resistance," SAE Paper 830720, April 1983.

[4]Stough, H. P., III, DiCarlo, D. J., and Patton, J. M., Jr., "Flight Investigation of the Effects of an Outboard Wing Leading-Edge Modification on Stall/Spin Characteristics of a Low-Wing, Single-Engine, T-Tail Light Airplane," NASA TP 2691, July 1987.

[5]Yip, L. P., King, P. M., Muchmore, C. B., and Davis, P., "Exploratory Wind Tunnel Investigations of the Low-Speed Stability and Control Characteristics of Advanced General Aviation Configurations," AIAA Paper 86-2596, Anaheim, CA, Oct. 1986.

[6]Hicks, R. M., Mendoza, J. P., and Bandettini, A., "Effects of Forward Contour Modification on the Aerodynamic Characteristics of the NACA 64(1)-212 Airfoil Section," NASA TM X-3293, 1975.

[7]Burk, S. M., Jr., and Wilson, C. F., Jr., "Radio-controlled Model Design and Testing Techniques for Stall/Spin Evaluation of General Aviation Aircraft," NASA TM 80510, April 1975.

[8]Fratello, D. J., Croom, M. A., Nguyen, L. T., and Domack, C. S., "Use of the Updated NASA Langley Radio-Controlled Drop-Model Technique for High-Alpha Studies of the X-29A Configuration," AIAA Paper 87-2559-CP, Monterey, CA, Aug. 1987.

[9]DiCarlo, D. J., Stough, H. P., III, Glover, K. E., Brown, P. W., and Patton, J. M., Jr., Development of Spin Resistance Criteria for Light General Aviation Airplanes," AIAA Paper 86-0812, Las Vegas, NV, April 1986.

[10]Stough, H. P., III, DiCarlo, D. J., and Patton, J. M., Jr., "Evaluation of Airplane Spin Resistance Using Proposed Criteria of Light General Aviation Airplanes," AIAA Paper 87-2562-CP, Monterey, CA, Aug. 1987.